

Cooperation without Coordination: Hierarchical Predictive Planning for Decentralized Multiagent Navigation

Rose E. Wang^{1,2}, J. Chase Kew¹, Dennis Lee¹, Tsang-Wei Edward Lee¹,
Tingnan Zhang¹, Brian Ichter¹, Jie Tan¹, Aleksandra Faust¹

Abstract—Decentralized multiagent planning raises many challenges, such as adaption to changing environments inexplicable by the agent’s own behavior, coordination from noisy sensor inputs like lidar, cooperation without knowing other agents’ intents. To address these challenges, we present *hierarchical predictive planning* (HPP) for decentralized multiagent navigation tasks. HPP learns prediction models for itself and other teammates, and uses the prediction models to propose and evaluate navigation goals that complete the cooperative task without explicit coordination. To learn the prediction models, HPP observes other agents’ behavior and learns to map own sensors to predicted locations of other agents. HPP then uses the cross-entropy method to iteratively propose, evaluate, and improve navigation goals, under assumption that all agents in the team share a common objective. HPP removes the need for a centralized operator (i.e. robots determine their own actions without coordinating their beliefs or plans) and can be trained and easily transferred to real world environments. The results show that HPP generalizes to new environments including real-world robot team. It is also 33x more sample efficient and performs better in complex environments compared to a baseline. The video and website for this paper can be found at <https://youtu.be/-LqgfksqNH8> and <https://sites.google.com/view/multiagent-hpp>.

I. INTRODUCTION

Consider a task where two or more robots need to perform a handover in obstacle-laden environments. Each robot needs to interpret their own noisy sensor inputs, decide where to meet the its teammate, and reliably navigate to the desired location. This is a more general formulation of an *Approach Task* [9] and *Rendezvous* [11] tasks. While other works address the reliable sensor-informed goal navigation [7], [10], the problem of determining the goal to navigate to is all but trivial. First, the communication between agents is often costly or technically challenging, rendering centralized planners difficult to use [3]. Second, without communication, each teammate needs to decide on the rendezvous point on its own, hoping that other teammates choose compatible points. The selection of a good rendezvous point depends on the obstacles in the environment, and on the policies and dynamics of the robots in the team. Take for example Fig. 1 where two agents must meet. Without communication, agents cannot pre-determine a meeting place and thus must coordinate in an ad-hoc manner [24] to converge to a meeting location. With an obstacle in the middle of the agents, the red agent could move to the left and the blue agent could move

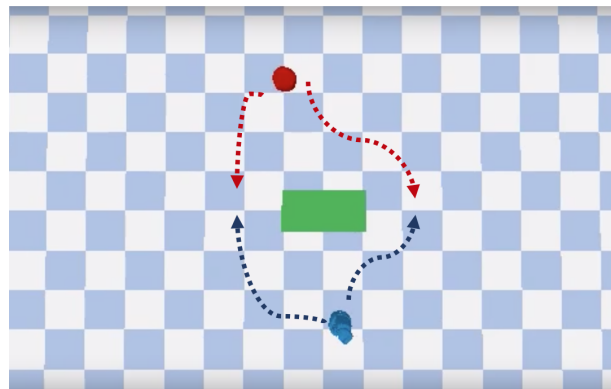


Fig. 1: Top down view of two robots (top, bottom) separated by obstacles (center) must meet each other. Both robots are decentrally controlled and there’s no communication. How should they move in order to meet? Example trajectories are illustrated in dashed arrows with the robot’s corresponding colors.

to the opposite side. A resolution to this miscoordinated situation depends on each agent’s ability to model other’s motions as well as adapt to diverging intentions using the limited information at hand.

The key challenges associated with solving the cooperative task without coordination for the real-world robot systems require modelling and adapting to other agents’ behavior. They require addressing questions, a) How should agents coordinate using only high-dimensional and imperfect sensor input, like lidar and localization? b) How should agents cooperate with others under partial observability (unable to observe the policies of other agents) and under uncertainty (unable to predict the intentions of other agents)? and c) How should agents adapt to nonstationarity (changing environments inexplicable by the agent’s own behavior)? These questions impact the performance of robot teams and the decision making process of each agent. The first two questions focus on the ability to model a dynamic environment and utilize the model for cooperation with limited knowledge of other agents. The last question deals with adaptively reacting to changes in the environment, for instance an agent decides to change its navigation goal. This component manifests in contemporary research on “ad hoc coordination” where teammates collaborate without prior agreement or commitments [24], and a robot’s policy might not capture how other agents will act in the world.

To address the above multiagent navigation challenges, we assume that all agents share a common objective, know each

¹ Robotics at Google, USA. ² Massachusetts Institute of Technology.

The research done during Wang’s internship at Robotics at Google. rewang@mit.edu, {jkew, ldennis, tsangwei, tingnan, ichter, jietan, faust}@google.com

teammate’s approximate location, and each agent knows how to navigate to a given, arbitrary location in the environment (e.g. has access to a control policy that maps sensors to actions). We present *hierarchical predictive planning* (HPP) for multiagent navigation tasks in decentralized navigation settings. HPP consists of a high and low-level planner. The high-level planner decides on the goals it believes are most likely to complete the shared team objective, and passes the goal to the lower level policy. The low-level control policy executes motion towards that goal until it receives a new goal. HPP addresses the three core questions stated in the introduction. First, *HPP* learns an approximate dynamics model of other robots in the team, directly from its own sensors via self-supervised learning; the dynamics models decouple the dynamics of the agents and of the task. Second, *HPP* maintains a goal distribution iterative updated with the cross-entropy method [8], a joint objective function, and the dynamics models, which simulate motion trajectories of each agent conditioned on a sampled goal. Third, *HPP* can replan using model predictions and adapt to the changes in the environment. The results show that HPP generalizes well to new environments (including operating on real, physical robots with zero-shot transfer), are up to 33 times more sample efficient than a centralized baseline, and outperform baseline in increasingly more complex settings.

The contributions of this work are a) the prediction models, which learn robot’s own and teammates’ dynamics by mapping own sensor information and robots’ poses to the next poses, and b) the model-based hierarchical planner, which proposes navigation goals that maximize the team’s objective, using only own observations and learned prediction models. Beyond robot rendezvous task, we believe this work is of interest to the larger multiagent community, as an example of a decentralized task with a shared objective, in realistic real-world setting with the noisy sensors, robot geometries, and imperfect controllers.

II. RELATED WORKS

Our work shares similar interests to recent deep multiagent reinforcement learning (MARL) works in that we strive towards decentralizing coordination and minimizing nonstationarity across agents. However, we achieve these goals through structural (hierarchy) and planning (model-based) means. Hierarchy allows agents to reason across abstract goals, which is useful for difficult navigation tasks where agents must converge on a meeting location in a partially observable environment. Deep learning allows us to learn models from high-dimensional sensors. Model-based methods can then use these models to plan with high-dimensional inputs. We use model-based planning as a mechanism to address uncertainty and nonstationarity.

Multiagent coordination: A popular paradigm in deep multiagent learning is that of centralized training and decentralized execution [22], [26], [13]. It extends the single-agent actor-critic framework [19] to a multiagent context where the centralized critic $Q(s, a)$ learns values of the observations and actions of *all agents* in the environment simultaneously.

Although centralized methods address the underpinning issue behind nonstationarity (capturing environment changes unexplainable by an agent’s own decentralized policy μ_i), the paradigm scales poorly with respect to the number of agents and observation sizes; our formulation theoretically scales linearly with respect to the number of agents. Attention mechanisms [17] have been explored for addressing this scalability issue, however it is unclear whether these methods could work with real robots where sensor observations like lidar are much larger than position and velocity vectors. Our work contributes a first comparison of a deep MARL algorithm running with real robot sensors and HPP, a method which learns decoupled dynamics from large sensor inputs.

Additionally, there exists a rich body of literature on multi-robot motion planning such as parallel motion planning [5], planning by decoupling the space and time coordination [12], or factorizing large multiagent Markov decision processes into efficient planning representations [15]. These propose efficient analysis and representations for planning in multiagent settings, however we address handling high dimensional sensors, which make learning agent and environment dynamics more difficult. Additionally, we address how to plan using learned (not ground truth) models.

Hierarchical and Model-Based Methods: The single-agent domain has explored hierarchical methods to integrate temporal abstractions as options (abstractions over the space of actions) [25]. These methods have also been used to find task commonality [21] or motion planning with nonlinear dynamics and uncertainty [18]. Our work extends upon these hierarchical methods for expressing and discovering multiagent goals abstracted in space. This idea is reminiscent of hierarchical option discovery [20], however we primarily focus on using hierarchy to achieve decentralized coordination and reduce the input space complexity of centralized operators.

We extend upon the recent single-agent advances in learning models through high-dimensional inputs and utilizing those models during planning (i.e. model-based reinforcement learning) [4]. In addition to learning with changes in sensor observations caused by other agents, we use model-based methods to address errors arising from multiagent nonstationarity. Previous works also used model-based methods for multiagent systems, e.g. simultaneously learning and utilizing the environment model to update a value function via prioritized sweeping [1]. We assume the agents can learn an approximate model a priori for online execution and error correction.

III. PROBLEM DEFINITION

To learn the cooperative *Approach task*, we base the problem definition on decentralized Markov Decision Processes (Dec-MDPs) [2]. The Dec-MDP, \mathcal{M} , is the tuple $\langle n, \mathcal{S}, \mathcal{O}, \mathcal{A}_{1..n}, T, \mathcal{R}, \gamma \rangle$. n is the number of agents. We assume the game theory notation i and $-i$ to mean agent i and all agents except i respectively. \mathcal{S} is a set of states describing the possible configurations for agents and objects in the environment. In this work, we assume the true state

space to be hidden and we do not explicitly model it. Joint observation space is $\mathcal{O} = [\mathcal{O}_1, \dots, \mathcal{O}_n]$, where \mathcal{O}_i is agent's i observations. Here, every agent observes the poses of all agents, own sensor observations, and relative goal position in polar coordinates, yielding $\mathbf{o}_i = [\mathbf{p}_i, \mathbf{p}_{-i}, \mathbf{o}_i^{(s)}, \mathbf{g}] \in \mathcal{O}_i$. Each pose consists of the global x (meters), global y (meters) and global heading (radians) information of the agent. $\mathcal{A}_{1\dots n}$ is the joint action space with $\mathbf{a}_i \in \mathcal{A}_i$ being the set of actions available to agent i . In this paper, the actions for each robot are robot's linear and angular velocities $\mathbf{a}_i = [v, \theta]$. Transition function $T : \mathcal{S} \times \mathcal{A}_{1\dots n} \times \mathcal{S} \rightarrow [0, 1]$ is a state distribution when transitioning from one state after agents take their respective actions $\mathbf{a}_{1\dots n}$. As with the true system state, we assume the transition function unobservable. Reward \mathcal{R} maps system state and action to a scalar that represents the collective reward function. Finally, $0 < \gamma < 1$ is the discount factor.

a) Single agent task: We assume that each agent is capable of single-agent navigation in an obstacle-laden environment. Specifically, we assume access to a goal-conditioned control policy π_i that maps agents' observations to actions $\pi_i(\mathbf{o}_i^{(s)}, \mathbf{g}) = \mathbf{a} \in \mathcal{A}_i$ for each agent, $i = 1 \dots n$. We call these policies point-to-point (P2P), and although in this paper we use the pre-trained policies from [7], any other method of driving a robot to a goal would be suitable, such as [10].

b) Approach Task: Formally, the *Approach task* requires n agents to cooperatively maximize the team reward, which is 1 if all agents meet within a predetermined distance, d from each other. We use the following reward, which is shared among all agents,

$$\mathcal{R}(\mathbf{p}_i, \mathbf{p}_{-i}, \mathbf{g}) = \mathbf{I}(|\mathbf{p}_j - \mathbf{p}_\mu| < d | \forall j \in \{i, -i\}, \mathbf{p}_\mu = \frac{1}{n} \sum_{k \in \{i, -i\}} \mathbf{p}_k) \quad (1)$$

where \mathbf{I} is an indicator variable, \mathbf{p}_μ is the center point of the robots' positions (average of their locations), and d is given value that controls the precision. Recall that i^{th} agent observation \mathbf{o}_i contains poses for all agents $\mathbf{p}_i, \mathbf{p}_{-i}$. Note that, as the agents become closer to each other the obstacle avoidance among them becomes more challenging, if not impossible, making the choice distance a non-trivial problem.

IV. METHODS

We now outline HPP, our hierarchical planning algorithm for *Approach task*. The algorithm conducts planning at two levels and is decentralized on *both* levels across agents. Figure 2 depicts the architecture at run-time. Each agent runs its own low-level and high-level policy. The high-level policy takes an agent's observations and recommends a goal for its low-level policy. Each low-level policy takes the recommended goal, sensor observation, and its own pose and outputs a control action to the robot. The only information shared between agents is their poses. The high-level policy recommends the next goal, taking into account what it believes the other agents would do if they shared the goal of completing the *Approach task*. To perform this reasoning, the high-level planner uses the prediction models to predict

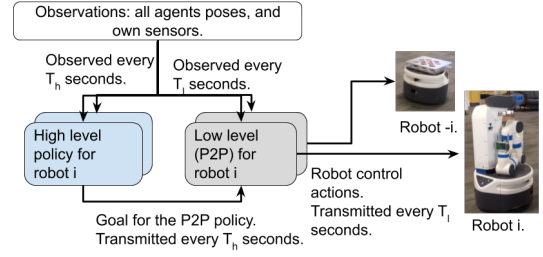


Fig. 2: HPP architecture at run-time. Each agent runs both high-level and low-level policies, but at different control frequencies. Both policies receive only their own agent's sensor information, and poses for all agents. The high-level policy produces a goal that is sent to the lower-level policy. The low-level policy computes the action for the agent i to perform. The low level policies are pre-trained and unaware of the multiagent setting. High-level policy proposes a goal *without* coordinating with other agents, based on its belief on the behavior given the shared task objective.



Fig. 3: Training environment with randomly filled obstacles used for training the dynamics prediction models $\mathbf{f}_i, \mathbf{f}_{-i}$. All agents (left, upper right) are given the same random goal (center) and move with their own P2P policies towards it.

trajectories and the predicted trajectories to evaluate goals against a joint team objective.

The rest of the section introduces the *prediction models* in Section IV-A) to approximate forward dynamics of agents, and then Section IV-B discusses *high-level* planning in detail.

A. Motion prediction models

Intuitively, the prediction models answer the following question, what would an agent do if it was trying to reach a goal? The key insight is that we can learn this predictive model by observing an agent performing a hidden policy. The key difficulty is that the agent that learns a prediction model does not have access to the sensory information of the agent under observation experiences. To that end, we learn two predictive models, *self-prediction*, \mathbf{f}_i , and *other-prediction* \mathbf{f}_{-i} . The self-prediction model maps agent's own sensors and goal to the difference of its next pose and sensors with respect to its own policy

$$\langle \Delta \mathbf{p}_i(t+1), \Delta \mathbf{o}_i^{(s)}(t+1) \rangle = \mathbf{f}_i(\mathbf{p}_i(t), \mathbf{o}_i^{(s)}(t), \mathbf{g}), \quad (2)$$

while the other-prediction model maps the agent's own sensors and goal to the difference of the other agent's next pose and this agent's lidar with respect to the other agent's



Fig. 4: Goal (g_0 and g_G) evaluation in the high-level policy Π . At the end of a simulated trajectory, the agents (left and right) are either a) far or b) close to each other. A goal reward is based on the negative final distance among agents. g_G is a better goal than g_0 because agents end up closer to each other.

policy,

$$\langle \Delta \mathbf{p}_{-i}(t+1), \Delta \mathbf{o}_i^{(s)}(t+1) \rangle = \mathbf{f}_{-i}(\mathbf{p}_{-i}(t), \mathbf{o}_i^{(s)}(t), \mathbf{g}). \quad (3)$$

Note, we do not store actions because we learn *goal-conditioned* dynamics. This alleviates having to know the exact action spaces of robots.

a) *Data collection*: Given blackbox P2P policies $\pi_i, i = 1 \dots n$ and a goal, all agents in the environment execute their P2P policies to move to that goal point. To provide diversification of the experience, we do domain randomization and instantiate the multiagent simulation environment with randomized obstacles (see Figure 3 for an example). For each agent, we collect two datasets \mathcal{D}_i and \mathcal{D}_{-i} that pose, sensor, and goal to the next pose:

$$\begin{aligned} \mathcal{D}_i &= [\langle \mathbf{p}_i(t), \mathbf{o}_i^{(s)}(t), \mathbf{g} \rangle, \langle \Delta \mathbf{p}_i(t+1), \Delta \mathbf{o}_i^{(s)}(t+1) \rangle] \\ \mathcal{D}_{-i} &= [\langle \mathbf{p}_{-i}(t), \mathbf{o}_i^{(s)}(t), \mathbf{g} \rangle, \langle \Delta \mathbf{p}_{-i}(t+1), \Delta \mathbf{o}_i^{(s)}(t+1) \rangle] \end{aligned}$$

.(t) is a trace of length h between timesteps $t-h$ and t .

b) *Model training*: The experiences \mathcal{D}_i and \mathcal{D}_{-i} are used to train a two different prediction models for each agent: *self-prediction*, \mathbf{f}_i , and *other-prediction* \mathbf{f}_{-i} . Both predictors are approximated with deep neural networks consisting of four fully connected layers, trained with mean squared loss.

B. Decentralized planner: high level policy

The decentralized planner Π_i uses 1 \mathbf{f}_i and $n-1$ \mathbf{f}_{-i} prediction models to evaluate and update a distribution over goals via the cross-entropy method [8]. Each agent, independently, simulates a fictitious centralized agent that fixes the goal of the agents: this goal pre-conditions the motion predicted by $\mathbf{f}_i, \mathbf{f}_{-i}$. Following the example from the introduction (Figure 1), this step is equivalent to evaluating the different navigation subgoals for each agent and selecting, for instance, the left side of the green rectangle as the goal the agent should navigate to and meet other agents. The planner selects a goal that maximizes reward, i.e. bringing the agents together.

Algorithm 1 describes the goal selection process that runs on an agent i . The goal selection process is iterative until convergence (Line 4). In the each iteration we sample the goal candidates from a Gaussian distribution. The distribution is initialized around the middle point of all agents and distribution variance is set to the variance in the poses (Line 2). Next (Lines 4-20), we improve on the proposed goal

(\mathbf{p}_μ). We sample N points from the distribution (Line 6) to generate goal candidates. For each proposed goal \mathbf{g}_j , the algorithm predicts the poses of all agents T timesteps in the future conditioned on \mathbf{g}_j (Lines 10-12), using sequential roll outs of the prediction models \mathbf{f}_i , and \mathbf{f}_{-i} (Lines 13-14). Finally, we evaluate the reward at the anticipated state of the system in the future using reward given in (1), and add the goal-reward pair to the evaluation set (Line 16). See Figure 4 for an illustration of how goal evaluations work. Once all the goals are evaluated, we select M goals with the highest reward (Line 18). Next, in Line 19, we propose a new goal, centered around the M selected most promising goals. Similarly, the variance of the new distribution is the variance of those M selected goals. We stop the process when the goals converge or we exceed maximum number of iterations. At that point, the algorithm returns the current center \mathbf{p}_μ of the distribution at Line 21.

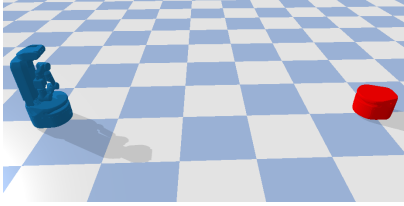
Algorithm 1 High level policy Π_i with cross-entropy method.

Input: $\mathbf{f}_i, \mathbf{f}_{-i}$, pre-trained prediction models
Input: T , rollout length; N , number of samples
Input: M , top number of samples for selection
Input: N_l , maximum number of iterations
Input: ϵ , cross-entropy method convergence criteria
Input: $\mathbf{o}_i = (\mathbf{p}_i, \mathbf{p}_{-i}, \mathbf{o}_i^{(s)}, \mathbf{g}_i)$, agent's observations
Output: \mathbf{g}_i , agent's navigation goal

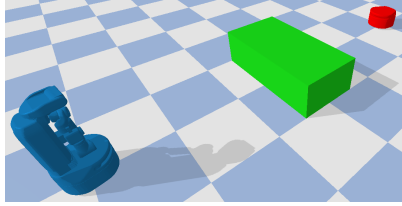
```

1: /* Initialize CEM parameters. */
2:  $\mathbf{p}_\mu \leftarrow \frac{1}{n} \sum_k \mathbf{p}_k, \mathbf{p}_\sigma \leftarrow \frac{1}{n} \sum_k (\mathbf{p}_k - \mathbf{p}_\mu)^2, k \in \{i, -i\}$ 
3:  $l \leftarrow 0$ 
4: while  $\epsilon < \mathbf{p}_\sigma$  and  $l < N_l$  do
5:   /* Sample N goals from current distribution. */
6:    $G = \{\mathbf{g}_j | \mathbf{g}_j \sim \mathcal{N}(\mathbf{p}_\mu, \mathbf{p}_\sigma^2), j \in [1 \dots N]\}$ 
7:    $R = \emptyset$  // Set of goal, reward pairs.
8:   /* Imagine how each goal plays out. */
9:   for all  $\mathbf{g}_j \in G$  do
10:    /* Initialize poses and sensors with the current. */
11:     $\hat{\mathbf{p}}_i \leftarrow \mathbf{p}_i, \hat{\mathbf{p}}_{-i} \leftarrow \mathbf{p}_{-i}, \hat{\mathbf{o}}_i^{(s)} \leftarrow \mathbf{o}_i, \tilde{\mathbf{o}}_i^{(s)} \leftarrow \mathbf{o}_i$ 
12:     $\Delta \mathbf{p}_i \leftarrow 0, \Delta \mathbf{o}_i^{(s)} \leftarrow 0, \Delta \hat{\mathbf{o}}_i^{(s)} \leftarrow 0, \Delta \tilde{\mathbf{o}}_i^{(s)} \leftarrow 0$ 
13:    /* Roll out with Eq. (2) and (3) */
14:    for  $k=1 \dots T$  do
15:       $\Delta \mathbf{p}_i, \Delta \hat{\mathbf{o}}_i^{(s)} \leftarrow \mathbf{f}_i(\hat{\mathbf{p}}_i + \Delta \mathbf{p}_i, \hat{\mathbf{o}}_i^{(s)} + \Delta \hat{\mathbf{o}}_i^{(s)}, \mathbf{g}_j)$ 
16:       $\Delta \mathbf{p}_{-i}, \Delta \tilde{\mathbf{o}}_i^{(s)} \leftarrow \mathbf{f}_{-i}(\hat{\mathbf{p}}_{-i} + \Delta \mathbf{p}_{-i}, \tilde{\mathbf{o}}_i^{(s)} + \Delta \tilde{\mathbf{o}}_i^{(s)}, \mathbf{g}_j)$ 
17:    end for
18:    /*  $\mathcal{R}$  computed using Eq. (1) */
19:     $R = R \cup (\mathbf{g}_j, \mathcal{R}(\hat{\mathbf{p}}_i, \hat{\mathbf{p}}_{-i}, \mathbf{g}_j))$ 
20:  end for
21:   $\hat{G} = \arg \max^M \{(\mathbf{g}, r) \in R\} // M \text{ goals w/ highest rewards.}$ 
22:   $\mathbf{p}_\mu \leftarrow \frac{1}{M} \sum_{\mathbf{p} \in \hat{G}} \mathbf{p}; \mathbf{p}_\sigma \leftarrow \frac{1}{M} \sum_{\mathbf{p} \in \hat{G}} (\mathbf{p} - \mathbf{p}_\mu)^2; l++ = 1$ 
23: end while
24: return  $\mathbf{p}_\mu$ 
```

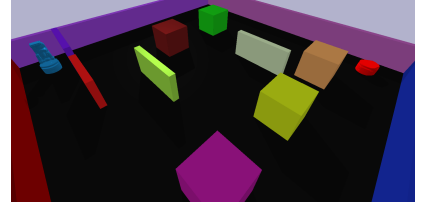
Finally, to run the HPP and complete a coordinated *Approach task* without coordination, each agent i runs an instance of the Π_i . The input to the Π_i is n prediction models, one self-prediction, and $n-1$ other agents prediction models, as each agent might be running a different P2P policy. Every other T_h timesteps, the Π_i observes its sensors and receives poses of all agents, and outputs a recommended goal for agent i . P2P policy receives the goal, and drives the



(a) Simple, no obstacle world.



(b) Wall world.



(c) Hard navigation world.

Fig. 5: Testing environments.

agent to the goal, performing actions every $T_l > T_h$ seconds. The process stops when the agents are close to each other or time runs out.

V. RESULTS

To evaluate HPP and the predictors on *Approach task*, we a) compare to another learning-based multiagent baseline, b) evaluate the prediction model accuracy, c) analyze how frequently goals should be selected and how far into the future we should predict, d) examine whether we can differentiate between a good goal sampling algorithm and a good prediction model, and e) demonstrate that the method transfers to a real robot system, closing the sim-to-real gap.

A. Setup

1) *Robot setup*: We use two robots, a Fetch and a Freight [27]. Each observes a 222 beam 2D lidar with 220 degree field of view to match the real robot sensors, as well as the global poses of all agents. Each agent’s action space is linear and angular base velocity, clipped to the ranges $[0, 1]$ meters/second and $[-3, 3]$ radians/second respectively. Linear acceleration is limited to 0.4 m/s^2 and angular acceleration to 1.48 rad/s^2 ($85^\circ/\text{s}^2$). The agent’s low-level policy operates every $T_l = 1$ steps and the high-level policy operates every $T_h = 10$ steps, unless otherwise specified. The episodes are $100 T_l$ timesteps (20 s) long both in training and in evaluation. In the real world experiments, the ROS navigation stack [23] provides the pose observations.

2) *Training setup*: Figure 3 shows the training environment for the predictive models f_i and f_{-i} , and Figure 5 three previously *unseen* test environments. The simulated evaluations are repeated 10 times where the agents are randomly initialized 5 meters from each other. The ϵ convergence criteria for CEM is 0.001. Episodes terminate when the agents are within 0.94 meters of each other (Fetch’s arm length) or after 20 s of sim time (100 timesteps) elapse.

3) *P2P policy setup*: The low-level policy was trained using AutoRL [7] with Soft Actor-Critic [16] and achieve 93% success at reaching a goal within 10 meters while avoiding collision with static obstacles. Its inputs are a stack of the last 5 observations of: log of the goal distance, goal heading, cosine and sine of goal heading, 220° lidar, and previous action. Its outputs are linear and angular velocities.



Fig. 6: Training loss for the i (self) and $-i$ (other) prediction models. Opaque lines are averaged over 100 steps.

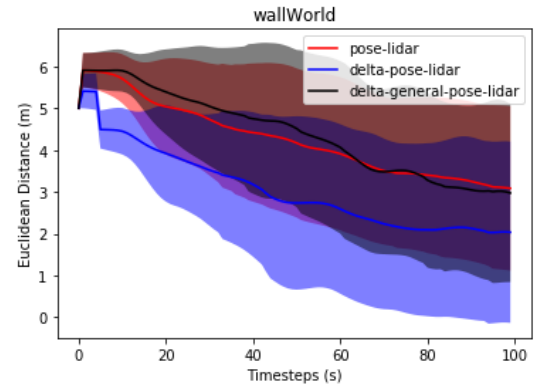


Fig. 7: Performance of HPP on wall world varying the prediction model. Lower is better. delta-pose-lidar (blue) is ours.

B. Prediction models evaluation

The prediction model is a 4-layer fully connected network with layer units 64, 128, 128 and 64 and a learning rate of 0.001. It is trained on experiences collected from an environment with randomized furniture obstacles (Figure 3). Goals are randomized within a 20×20 meter square and are not guaranteed to be collision-free. The history trace length, H , is 5 for all agents. Low-level policies navigating towards randomly selected goals collect 50,000 trajectories, or the equivalent of the about 11 days of real-time experience. Each prediction model (f_i, f_{-i}) has its own trained network, trained on 50,000 epochs with batch sizes of 500. The data collection and training take about 3 hours to complete.

Both *self-prediction* and *other-prediction* models converge (Fig. 6). As expected, *self-prediction* is easier than predicting another agent’s motion without having its sensor readings.

What attributes make a good prediction model? We

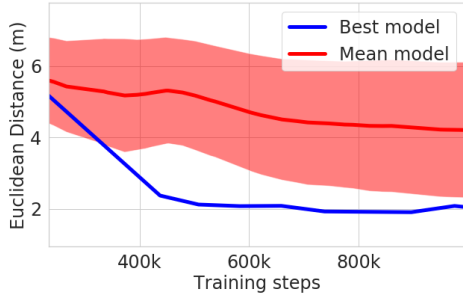


Fig. 8: MADDPG training curves. The pink shaded region shows the standard deviation across a batch of training runs. The blue curve is the best trained MADDPG model, which use as the baseline.

conduct an ablation study on model representations for f_i, f_{-i} . To contrast prediction methods, we train two additional prediction types under the same settings and inputs. We refer to the prediction type presented in Section IV-A as delta-pose-lidar. The two additional ones are pose-lidar and delta-general-pose-lidar. pose-lidar directly outputs the next pose and lidar predictions. delta-general-pose-lidar differs from delta-pose-lidar in that it predicts the pose of agent $-i$ relative to the current pose of agent i , and predicts the full lidar observation of agent i . We evaluate the task performance of the prediction models on wall world (Fig. 5b).

Fig. 7 shows that delta-pose-lidar performs the best while the other two prediction models perform equally well. In particular, the first few timesteps indicate a drastic decrease in euclidean distance since these agents quickly overcome the symmetry-breaking problem presented in wall world. Future work can investigate different prediction schemes.

C. HPP evaluation

To assess HPP performance we compare to MADDPG [22]. We choose MADDPG as a baseline instead of COMA [13] or MAAC [17] because it is an off-policy method, and our environment is much more expensive for data collection than a particle environment (used in MADDPG). Both the policy and critic networks are two layer networks with 64 units in each. Batch size is 1024 and learning rate is 0.0005.

Training sample efficiency: Training our model predictors f_i and f_{-i} is more sample efficient than training MADDPG. The model predictors converge after 30k steps of training (Fig. 6), while MADDPG takes 1M steps to converge (Fig. 8). MADDPG is also relatively unstable; of 10 policies, 3 failed to converge, while the predictors are stable to train.

Generalization and performance evaluation: To evaluate HPP generalization, we assess both HPP and MADDPG in the three evaluation environments (Fig.5). HPP brings the agents close together in all three environments within a consistent timeframe (60 steps), although in the environments with obstacles the agents end up somewhat farther apart than in the empty environment (Fig. 9). This is to be expected,

as the task becomes more difficult because the agents must balance their goals against avoiding collisions.

Interestingly, MADDPG generalizes better to domains that are unlike the training environment: it performs well in the simple and wall worlds, which are least alike to the very cluttered training environment. We hypothesize that MADDPG learns to primarily use the poses in the observation to determine actions, thus it performs well on obstacle-minimal environments. However, it does not learn how to use lidar, a high-dimensional input with much less structure than poses, to navigate in structured obstacle-filled environments. This may be attributable to the algorithm’s centralized training procedure, which equally considers all inputs without distinguishing observations of environment dynamics (learned through lidar) from observations of agent dynamics (learned through pose information). In the simple world (Fig. 11a), MADDPG outperforms HPP. In the wall world, HPP and MADDPG perform comparably (Fig. 11b). However, in the most complex, nav world, MADDPG fails completely, while HPP performs well (Fig. 11c).

In summary, the evidence suggests that HPP is more sample-efficient than MADDPG, and it is more beneficial to use it in more complex environments.

D. Planning hyper-parameters evaluation

We now investigate the role of three planning hyper-parameters in Algorithm 1: planning frequency (T_h), planning horizon (T), and goal sampling parameters.

Planning frequency: Across the three environments, planning every 5 timesteps leads to faster task completion compared to every 10 or 15 timesteps (Fig. 10). Though this is unsurprising, we also note that planning frequency makes more difference in more complex environments. However, frequent planning comes at the cost of higher computational load, so it is helpful to tune it to the desired precision. Figure 10 suggests that the optimal planning rate depends on the environment, so planning rate should be tuned once per environment.

Planning horizon: Shorter planning horizons (fewer rollout steps) result in faster planning. The evidence in Fig. 11 suggests that the performance gap does not depend on the environment, as it consistently affects planning accuracy across all environments. This means that we should tune the planning horizon—based on the desired planning accuracy—just once for the predictor model and use it for all environments.

Goal sampling parameters Finally, we conducted experiments where we varied the parameters of the cross-entropy method: maximum number of iterations, number of goals sampled G , and number of top goals used for updating the CEM distribution. None of these ablation experiments indicated that HPP has a strong dependency on the goal sampling parameters.

E. Experiment on real robots

We did sim-to-real zero-shot transfer of HPP into real world environments, some similar to those in simulation

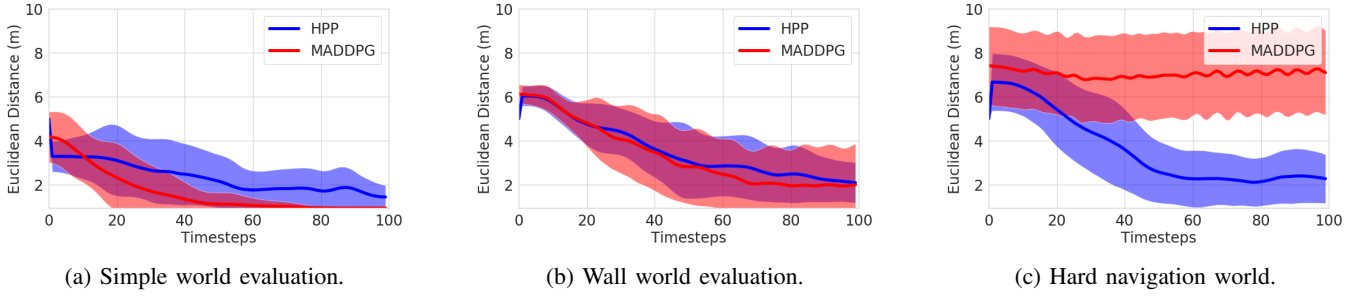


Fig. 9: Distance between agents over time, as compared with MADDPG.

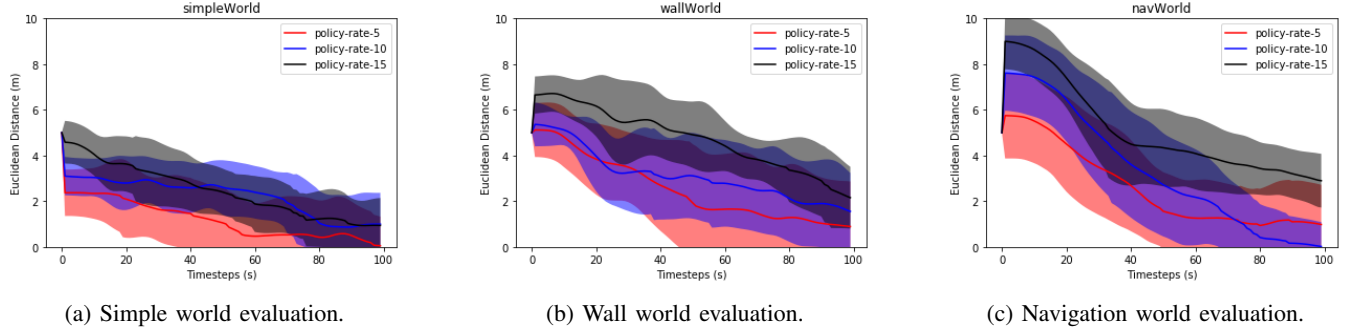


Fig. 10: Planning frequency at which the high level policy II recalculates new goal across environments. Lower is better. The planning frequency should be tuned per environment.

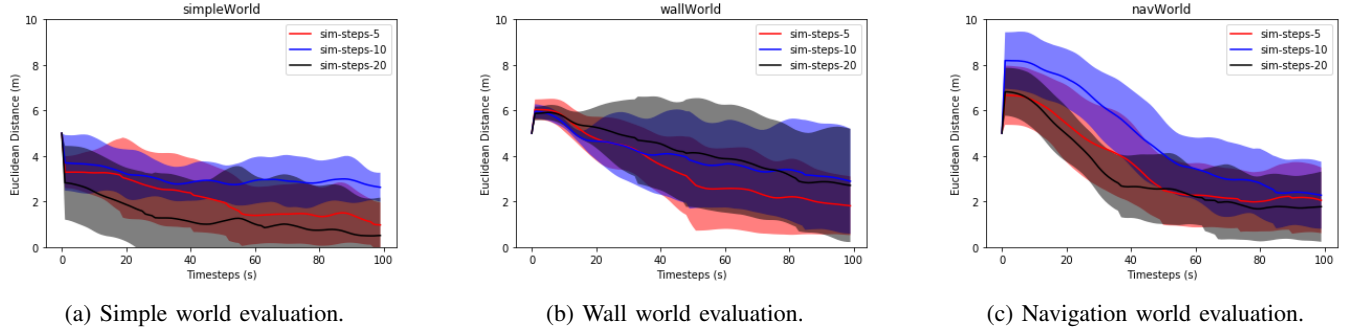


Fig. 11: Planning horizon evaluations across environments. Lower is better. Planning horizon does not depend on the environment, and should be tuned once per predictor.

and some novel (see attached video). The actions of the real robots are not synchronized in any way. They are planned and executed independently. HPP is able to handle the noisiness of real robotic sensors and also to handle the latency in communication networks. This is partly because HPP leverages low-level P2P policies' strengths – trained with noise and transfer well to the real world [7], [14].

VI. DISCUSSION

HPP offers *modularity* in combining both model-free and model-based methods for decentralizing navigation. Its hierarchical design provides powerful abstractions for multi-agent coordination to perform more sample-efficient learning. A key component in HPP is the *generalizability* of the prediction models f_i, f_{-i} . Trained on environments with randomly placed obstacles, the prediction models are capable of making reliable rollouts in evaluation environments that

help select useful goals. This is an ideal feature to have in any system, but especially in multiagent systems where inferring other agents' intentions is a difficult challenge.

The combination of the *modularity* and *generalizability* enables real-world complex multiagent planning. Prior works have used P2P policies as building blocks [14] and learned reliable predictors of one's own dynamics [6]. This work goes two steps further. First, it demonstrates that agents can learn to anticipate other agents' behaviors (governed by hidden policies) merely by observing them. Second, it uses those predictions to solve complex, cooperative, real-world, multiagent tasks *without explicit coordination*.

As a future extension to this work, we hope to investigate the scalability of this approach to three or more agents. For agents up to 5, we imagine the CEM rollouts would be parallelizable and thus would require no more time than

















Environment type	1	2	3	4
Simple				
Wall				
Forest				
Forest				

TABLE I: Images from real world evaluations on environment configurations.

currently. For more agents, future work could consider using similar parallelization methods or aggregating the motions of other agents (group dynamics) instead of modelling them individually (many individual dynamics).

VII. CONCLUSIONS

This work proposes *hierarchical predictive planning* (HPP), a hierarchical, model-based method for enabling multiple agents to coordinate in a decentralized manner using high-dimension observations (such as lidar observations) and minimal communication among agents. We show that the prediction models are capable of generalizing to unseen environments both in simulation and in the real world. The hierarchical planner combined with the prediction models enable for decentralized cooperation with sample-efficient means, both in simulation and in the real world.

ACKNOWLEDGMENTS

We thank Michael Everett, Oscar Ramirez and Igor Mordatch for the insightful discussions.

REFERENCES

- [1] A. Akramizadeh, A. Afshar, M. B. Menhaj, and S. Jafari. Model-based reinforcement learning in multiagent systems with sequential action selection. *IEICE TRANSACTIONS on Information and Systems*, 94(2):255–263, 2011.
- [2] D. S. Bernstein, R. Givan, N. Immerman, and S. Zilberstein. The complexity of decentralized control of markov decision processes. *Mathematics of operations research*, 27(4):819–840, 2002.
- [3] L. Brunet, H.-L. Choi, and J. How. Consensus-based auction approaches for decentralized task assignment. In *AIAA guidance, navigation and control conference and exhibit*, page 6839, 2008.
- [4] J. Buckman, D. Hafner, G. Tucker, E. Brevdo, and H. Lee. Sample-efficient reinforcement learning with stochastic ensemble value expansion, 2018.
- [5] D. Challou, M. Gini, V. Kumar, and C. Olson. Very fast motion planning for dexterous robots. In *Proceedings. IEEE International Symposium on Assembly and Task Planning*, pages 201–206. IEEE, 1995.
- [6] H.-T. L. Chiang, J. Hsu, M. Fiser, L. Tapia, and A. Faust. Rl-rrt: Kinodynamic motion planning via learning reachability estimators from rl policies. *IEEE Robotics and Automation Letters*, 4(4):4298–4305, 2019.
- [7] L. Chiang, A. Faust, M. Fiser, and A. Francis. Learning navigation behaviors end-to-end with autolr. 4(2):2007–2014, April 2019.
- [8] P.-T. De Boer, D. P. Kroese, S. Mannor, and R. Y. Rubinstein. A tutorial on the cross-entropy method. *Annals of operations research*, 134(1):19–67, 2005.
- [9] H. Durrant-Whyte and T. Bailey. Simultaneous localization and mapping: part i. *IEEE robotics & automation magazine*, 13(2):99–110, 2006.
- [10] T. Fan, X. Cheng, J. Pan, P. Long, W. Liu, R. Yang, and D. Manocha. Getting robots unfrozen and unlost in dense pedestrian crowds. *IEEE Robotics and Automation Letters (RA-L)*, 2019.
- [11] A. Faust, N. Malone, and L. Tapia. Preference-balancing motion planning under stochastic disturbances. In *Proc. IEEE Int. Conf. Robot. Autom. (ICRA)*, pages 3555–3562, 2015.
- [12] C. Ferrari, E. Pagello, J. Ota, and T. Arai. Multirobot motion coordination in space and time. *Robotics and autonomous systems*, 25(3-4):219–229, 1998.
- [13] J. Foerster, G. Farquhar, T. Afouras, N. Nardelli, and S. Whiteson. Counterfactual multi-agent policy gradients, 2017.
- [14] A. Francis, A. Faust, H.-T. L. Chiang, J. Hsu, J. C. Kew, M. Fiser, and T.-W. E. Lee. Long-range indoor navigation with prm-rl. 2020.
- [15] C. Guestrin, D. Koller, and R. Parr. Multiagent planning with factored mdps. In *Advances in neural information processing systems*, pages 1523–1530, 2002.
- [16] T. Haarnoja, A. Zhou, P. Abbeel, and S. Levine. Soft actor-critic: Off-policy maximum entropy deep reinforcement learning with a stochastic actor, 2018.
- [17] S. Iqbal and F. Sha. Actor-attention-critic for multi-agent reinforcement learning. *arXiv preprint arXiv:1810.02912*, 2018.
- [18] A. Jain and S. Niekum. Efficient hierarchical robot motion planning under uncertainty and hybrid dynamics, 2018.
- [19] V. R. Konda and J. N. Tsitsiklis. Actor-critic algorithms. In *Advances in neural information processing systems*, pages 1008–1014, 2000.
- [20] A. S. Lakshminarayanan, R. Krishnamurthy, P. Kumar, and B. Ravindran. Option discovery in hierarchical reinforcement learning using spatio-temporal clustering, 2016.
- [21] Z. Li, A. Narayan, and T.-Y. Leong. An efficient approach to model-based hierarchical reinforcement learning. In *Thirty-First AAAI Conference on Artificial Intelligence*, 2017.
- [22] R. Lowe, Y. Wu, A. Tamar, J. Harb, P. Abbeel, and I. Mordatch. Multi-agent actor-critic for mixed cooperative-competitive environments, 2017.
- [23] M. Quigley, K. Conley, B. P. Gerkey, J. Faust, T. Foote, J. Leibs, R. Wheeler, and A. Y. Ng. Ros: an open-source robot operating system. In *ICRA Workshop on Open Source Software*, 2009.
- [24] P. Stone, G. A. Kaminka, S. Kraus, and J. S. Rosenschein. Ad hoc autonomous agent teams: Collaboration without pre-coordination. In *Twenty-Fourth AAAI Conference on Artificial Intelligence*, 2010.
- [25] R. S. Sutton, D. Precup, and S. Singh. Between mdps and semi-

mdps: A framework for temporal abstraction in reinforcement learning. *Artificial intelligence*, 112(1-2):181–211, 1999.

- [26] R. E. Wang, M. Everett, and J. P. How. R-maddpg for partially observable environments and limited communication. 2019.
- [27] M. Wise, M. Ferguson, D. King, E. Diehr, and D. Dymesich. Fetch and freight: Standard platforms for service robot applications.